ELECTRONIC SUPPLEMENTARY INFORMATION

An intensified π-hole in beryllium-doped boron nitride meshes: its determinant role in CO_2 conversion into hydrocarbon fuels

Luis Miguel Azofra, Douglas R. MacFarlane and Chenghua Sun*

ARC Centre of Excellence for Electromaterials Science (ACES), School of Chemistry, Faculty of Science, Monash University, Clayton, VIC 3800, Australia

*Author to whom correspondence should be addressed:

CS. Tel: (+61) 3 9902 9916; Fax: (+61) 3 9905 4597; E-mail: Chenghua.Sun@monash.edu

---

	Pages
Computational Details	S2
Fig. S1. MEP for selected doped BNs	S3
Fig. S2. Binding/reaction energies for the *CO_2 and OCHO• steps catalysed by Be-doped BNs	S4
Fig. S3. Minimum energy path for the CO_2 conversion mechanism catalysed by pure BNs	S5
Fig. S4. Different intermediate structures calculated in the full exploration of the CO_2 conversion mechanism catalysed by Be-doped BNs	S6
Fig. S5. Detailed view of the reaction site structures in Be-doped BNs	S7
Table S1. Electronic energies	S8
Fig. S6. Effect of explicit H_2O molecules in the CO_2 conversion mechanism	S9
References	S11

Computational Details

The CO_2 electrochemical conversion mechanism catalysed by beryllium-doped boron nitride nano-meshes or sheets (BNs) has been studied by means of density functional theory (DFT) through the generalised gradient approximation (GGA) with the Perdew-Burke-Ernzerhof (PBE) functional,[1] using a plane-wave cut-off energy of 450 eV.[2] Concerning the periodic boundary conditions, the Brillouin zone was sampled by 3×3×1 *k*-points using the Monkhorst-Pack scheme. In order to avoid interactions between periodic images, a vacuum distance of 20 Å was imposed between different layers. At first stage, optimisation calculations were done using energy and force convergence limits equal to 10^{-4} eV/atom and |0.01| eV/Å, respectively, and 0.5 fs time-steps were applied for ion-motion. Finally, with the aim to obtain more accurate values, thresholds for energy and time-steps for ion-motion were decreased to 10^{-6} eV/atom and 0.02 fs, in each case, and zero point energy (ZPE) and vibrational contributions for the entropy ($-TS_{vib}$) were calculated for electronic energy corrections at such level. All optimisation calculations have been performed through the facilities provided by the Vienna *Ab-Initio* Simulation Package (VASP, version 5.3.3).[3]

The analysis of the maxima and minima on the molecular electrostatic potential (MEP) on the 0.001 a.u. electron density iso-surface has been performed with the WFA-SAS program[4] over representative quantum dots at the PBE0[1]/6-31+G(d)[5] computational level, previously optimised and corroborated their condition of minima in the potential energy surface (PES) through the calculation of the vibrational frequencies *via* the Gaussian09 (revision D.01) package.[6]

Eqn. (1) has been applied to show the reaction energies, where *n* is the number of H^+/e^- pairs transferred and *m* the number of H_2O molecules released, if applicable. In this context, Nørskov and co-workers[7] estimate that the chemical potential of the H^+/e^- pair has the half value of the chemical potential of the dihydrogen (H_2) molecule [see Eqn. (2)]:

$$\Delta G_R = G(\text{surface}\cdots CO_{2-m}H_{n-2m}) + m\, G(H_2O) - G(\text{surface}) - G(CO_2) - \tfrac{n}{2}\, G(H_2) \quad (1)$$

$$\mu(H^+ + e^-) = \tfrac{1}{2}\, \mu(H_2) \quad (2)$$

Figure S1. Preliminary evaluation of the molecular electrostatic potential (MEP) for different doped BN quantum dots calculated at DFT level, using the Grimme's B97-D functional[8] and the 6-31+G(d) and 3-21G Pople's basis sets for the heavy and hydrogen atoms, respectively.[5] Models have been built in basis to pnictogen (P, As), tetrel (C, Si, and Ge), chalcogen (O, S, and Se), and Be substitutions. Yellow contours represent positive MEP iso-values (0.05 a.u.). The prominence of the positive lobes indicates plausible/strength binding points with negative entities of partner molecules.

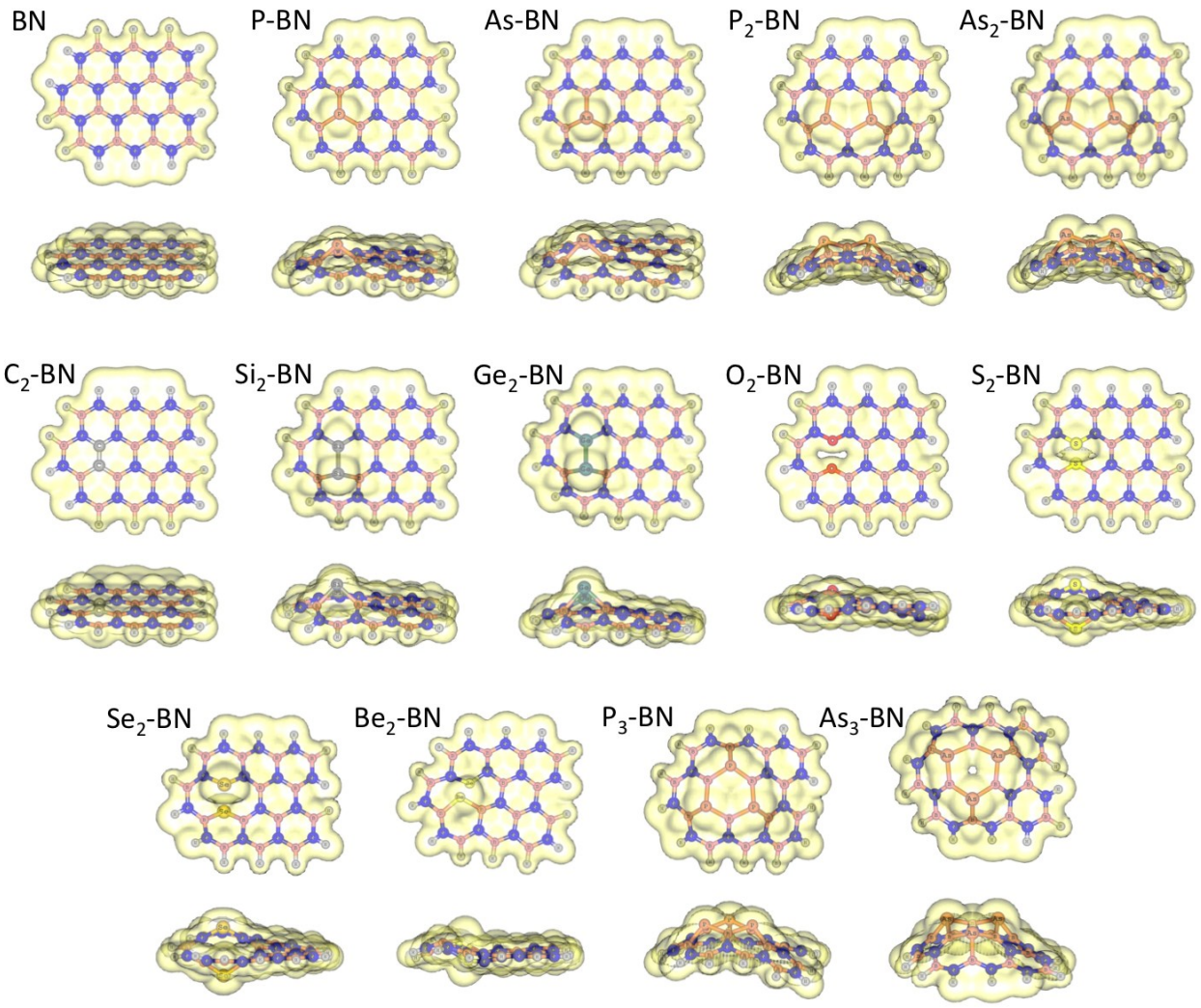

Figure S2. Binding/reaction energies for the $*CO_2$ and OCHO• steps, catalysed by representative pure BN, g-C_3N_4, and Be-doped BN quantum dots. Direct relationships can be seen between the binding/reaction energies and the deep of the π-holes (see main text). Calculations at PBE0/6-31+G(d) computational level.

	$*CO_2$			OCHO•		
	ΔE + ZPE	ΔH	ΔG	ΔE + ZPE	ΔH	ΔG
BN	–0.05	–0.01	0.13	2.32	2.32	2.76
g-C_3N_4	–0.39	–0.37	–0.03	2.00	1.98	2.54
Be-doped BN	–0.46	–0.46	–0.07	–1.43	–1.52	–0.78

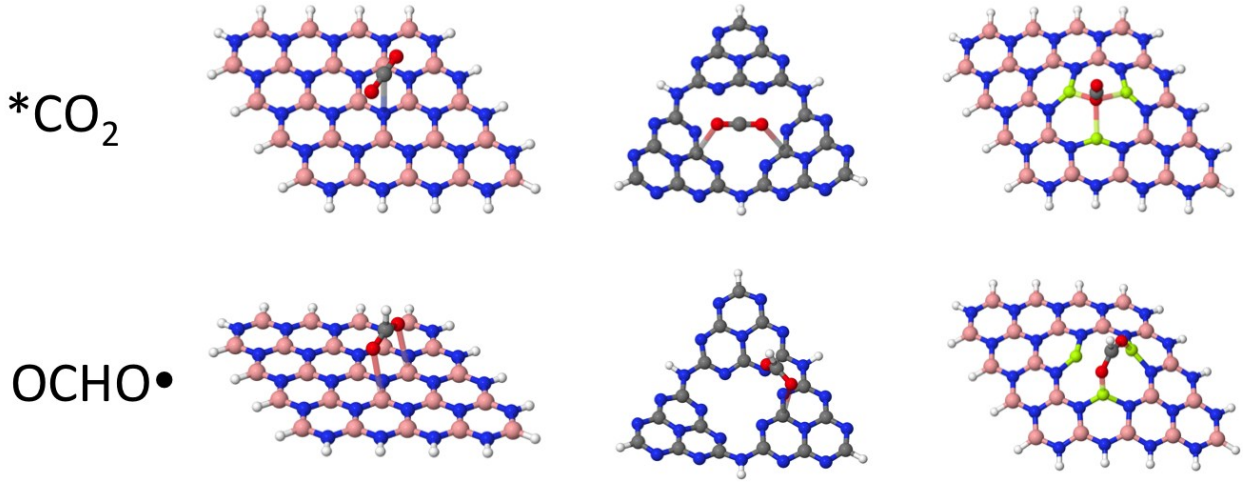

Figure S3. Minimum energy path corresponding to the CO_2 conversion mechanism catalysed by pure BNs. Relative reaction Gibbs free energies at 298.15 K (not including ZPE and thermal corrections) are indicated in eV. Calculations have been performed with similar settings than the applied for the analysis of the CO_2 conversion mechanism catalysed by Be-doped BNs. (See **Computational Details** above).

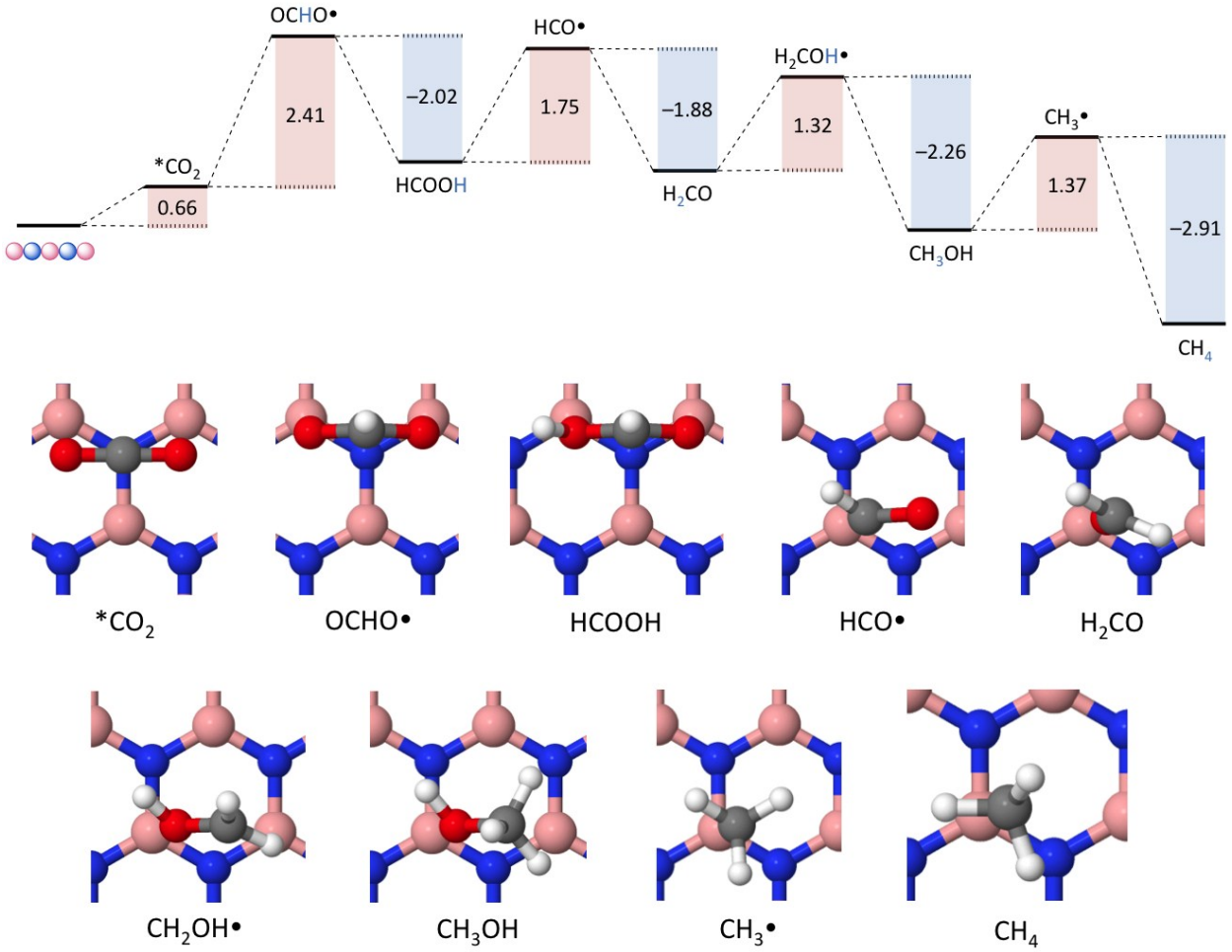

Figure S4. Different intermediate structures calculated in the full exploration of the CO_2 conversion mechanism catalysed by Be-doped BNs. Relative Gibbs free energies at 298.15 K are indicated in eV (thermal and ZPE corrections applied). It is hypothesised that Be-doped BNs are non-selective towards the formation of formic acid (HCOOH).

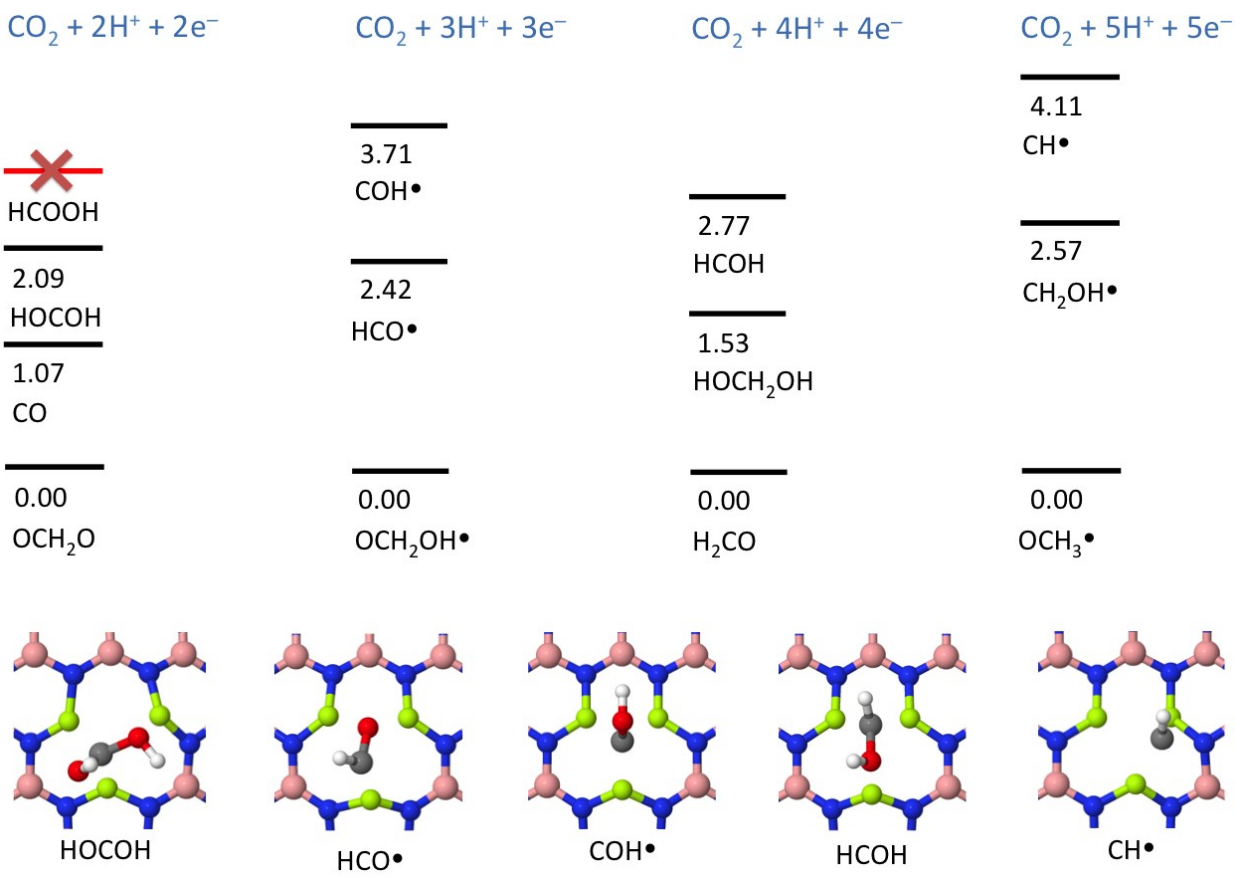

Figure S5. Detailed view of the reaction site structures in Be-doped BNs. Dashed orange lines indicate the link between two proximal atoms from the substrate and the mesh moieties, respectively. Selected interatomic distances are shown in Å.

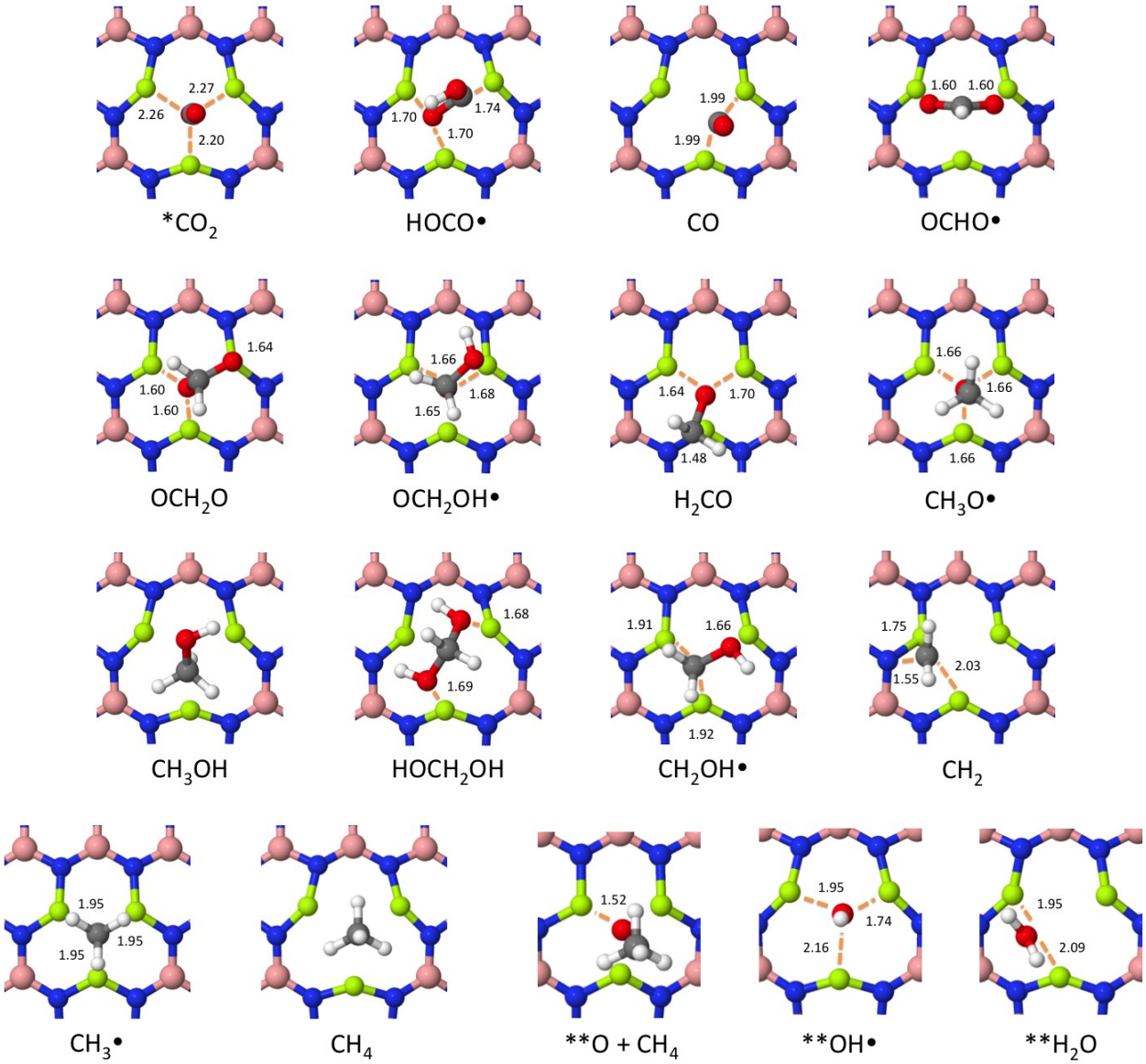

Table S1. Gibbs free energies (thermal and ZPE corrections applied), in eV, corresponding to the isolated CO_2, H_2, H_2O, and CH_4 species and the different states along the CO_2 conversion mechanism catalysed by Be-doped BNs. (See **Computational Details** above).

Species	*G*
CO_2 (*g*)[a]	–23.36
H_2 (CHE)[a]	–6.85
H_2O (*g*)[a]	–14.28
CH_4 (*g*)[a]	–23.44

Species	*G*	Species	*G*	Species	*G*
Clean surface	–407.62	H_2CO	–432.91	CH_4	–431.41
*CO_2[b]	–431.44	CH_3O•	–437.00	**O + CH_4[b]	–440.96
HOCO•	–435.03	CH_3OH	–437.49	**OH•[b]	–421.57
CO	–423.78	$HOCH_2OH$	–445.66	**H_2O[b]	–425.74
OCHO•	–435.84	CH_2OH•	–434.43		
OCH_2O	–439.13	CH_2	–423.44		
OCH_2OH•	–443.64	CH_3•	–428.08		

[a]E_{elec} – T*S* + ZPE, data obtained by Peterson *et al.*[7] and Lim and co-workers.[9] T = 298.15 K. Assumed fugacity: 101,325 Pa for the CO_2 (*g*) and H_2 (CHE) species, 20,467 Pa for CH_4 (*g*), and 3,534 Pa for H_2O (*g*). Since $\int C_P\,dT$ is almost negligible and $\Delta\int C_P\,dT \approx 0$ eV, no thermal corrections for the enthalpy have been take into account for the *G* estimation. For clean surface and adsorbates, $-TS \approx -TS_{vib}$.

[b]Physisorbed and chemisorbed species are indicated as * and **, respectively. The alternative path towards the formation of methane by oxygenation on the surface and the subsequent hydrogenation to produce one H_2O molecule is highlighted in blue colour font.

Figure S6. Effect of explicit H_2O molecules (three and six) in the CO_2 conversion mechanism into CH_4 (methanediol path) catalysed by Be-doped BNs.[a] Relative reaction Gibbs free energies at 298.15 K (not including ZPE and thermal corrections) are indicated in eV. (See **Computational Details** above).

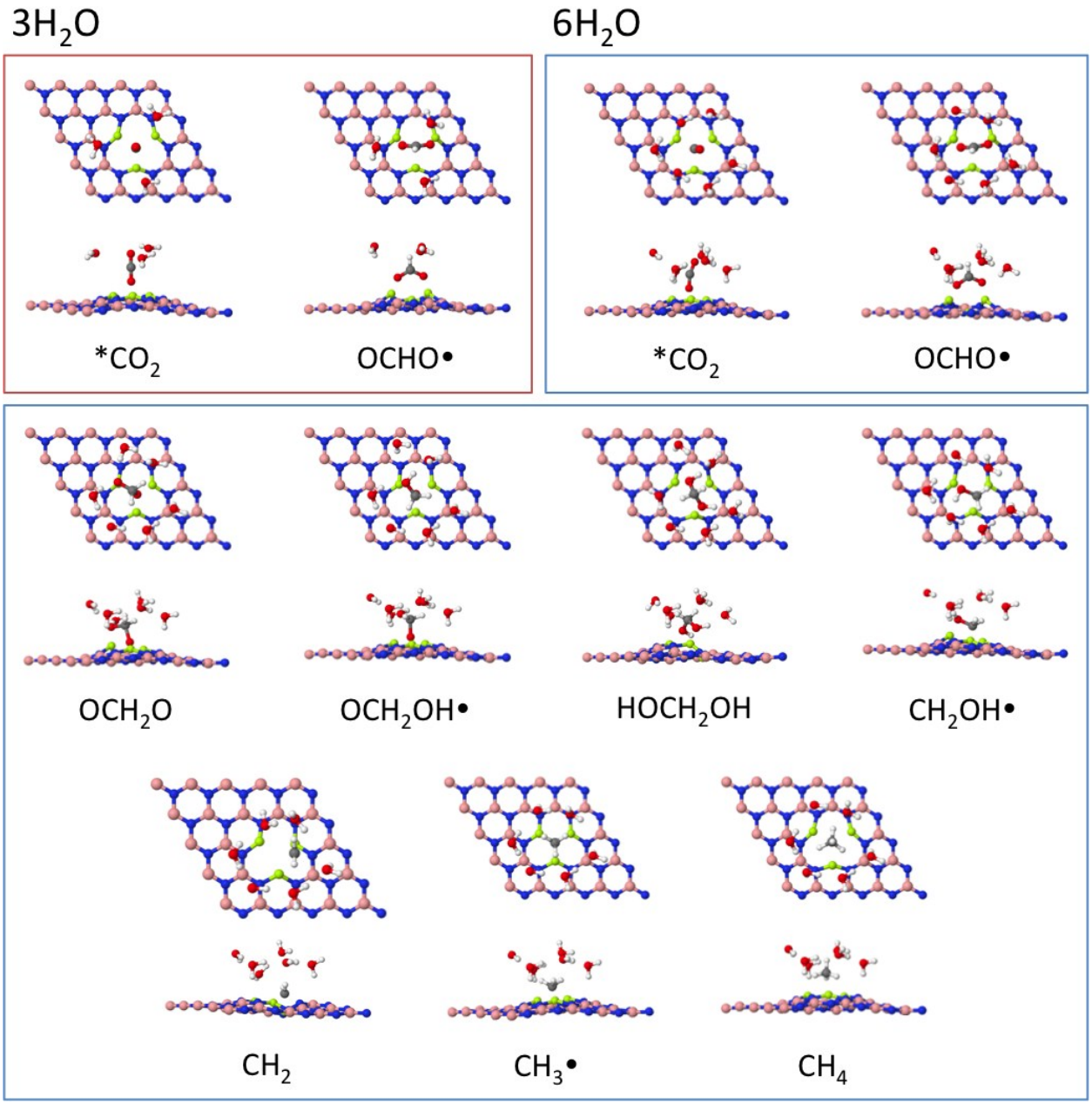

[a]Plane-wave cut-off energy of 400 eV, Brillouin zone sampled by 3×3×1 *k*-points using the Monkhorst-Pack scheme, energy and force convergence limits equal to 10^{-4} eV/atom and |0.05| eV/Å (|0.06| eV/Å for the $*CO_2$ step when optimised with six explicit H_2O molecules) respectively, and 0.5 fs time-steps for ion-motion.

Two models have been investigated for the analysis of the inclusion of explicit H_2O molecules along the reaction path. On the one hand, three H_2O molecules were placed surrounding the adsorbates. On the other, six H_2O molecules were introduced, starting from the optimised geometries when using three and placing the other three in an inner layer interacting with both the surface and the adsorbates.

Species	ΔG^a ($3H_2O$)	ΔG^a ($6H_2O$)	ΔG ($0H_2O$)
$*CO_2$	–0.53	–0.19	–0.45
HOCO•	–1.13	–0.60	–0.98
OCH_2O	–0.22	–0.19	0.14
OCH_2OH•	–1.42	–1.29	–1.09
$HOCH_2OH$	1.52	1.13	1.41
CH_2OH•	0.43	0.19	0.37
CH_2	0.22	0.41	0.14
CH_3•	–1.46	–1.40	–1.22
CH_4	0.42	0.48	0.10

When comparing the test results for both cases in which explicit H_2O molecules have been included with the one obtained for the isolated CO_2 conversion mechanism into CH_4 (methanediol path), no huge differences can be seen. In fact, a linear relationship is described for ΔG in both cases, being specially correlated when using three explicit H_2O molecules (R^2 = 0.97) than when using six (R^2 = 0.88). Table attached.

As previously corroborated, the single H_2O adsorption is thermodynamically preferred than the CO_2 fixation, however, once CO_2 is linked on the surface, the presence of H_2O molecules as solvent still indicates its spontaneous physisorption, notwithstanding, a paradigmatic bending of CO_2 (162 deg) is observed in the labelled as $6H_2O$ model. As happened with the $*CO_2$ step, the first hydrogenation step seems to be more spontaneously reduced in terms of the Gibbs free energy for the $3H_2O$ model, however, in the $6H_2O$ model this value decreases to –0.60 eV, but newly displaying spontaneous energies. Moreover, the OCH_2O, OCH_2OH•, $HOCH_2OH$, and CH_2OH• production are stabilised by a decrease of the reaction energies along the second, third, fourth, and fifth H^+/e^- gains, respectively, by effect of six H_2O; the production of CH_4 becomes less spontaneous, which seems obvious due to the intrinsic hydrophobic behaviour of this hydrocarbon compound. (See Table attached). Interesting conclusions can be advanced for the limiting step of this selected path, corroborating in all the cases that it is the production of methanediol. The $6H_2O$ model establishes a value up to 1.13 eV, while for the original (zero) and $3H_2O$ models they are 1.41 and 1.52 eV, respectively. Such stabilisation can be explained for the presence of H-bonds between the adsorbed $CH_2(OH)_2$ species and the six H_2O molecules, however what seems to be a controversy in the $3H_2O$ model can be explained due to the poor

hydration exerting for only three explicit H_2O molecules, leading to structural artifacts. Thus, the inclusion of more explicit H_2O molecules as in the $6H_2O$ model seems more convenient, allowing a better description of the systems under study.

References

1. (a) J. P. Perdew, K. Burke and M. Ernzerhof, *Phys. Rev. Lett.*, 1996, **77**, 3865; (b) J. P. Perdew, K. Burke and M. Ernzerhof, *Phys. Rev. Lett.*, 1997, **78**, 1396.
2. (a) P. E. Blöchl, *Phys. Rev. B*, 1994, **50**, 17953; (b) G. Kresse and D. Joubert, *Phys. Rev. B*, 1999, **59**, 1758.
3. (a) G. Kresse and J. Hafner, *Phys. Rev. B*, 1993, **47**, 558; (b) G. Kresse and J. Hafner, *Phys. Rev. B*, 1994, **49**, 14251; (c) G. Kresse and J. Furthmüller, *Comput. Mat. Sci.*, 1996, **6**, 15; (d) G. Kresse and J. Furthmüller, *Phys. Rev. B*, 1996, **54**, 11169.
4. F. Bulat, A. Toro-Labbé, T. Brinck, J. Murray and P. Politzer, *J. Mol. Model.*, 2010, **16**, 1679.
5. M. J. Frisch, J. A. Pople and J. S. Binkley, *J. Chem. Phys.*, 1984, **80**, 3265.
6. M. J. Frisch, G. W. Trucks, H. B. Schlegel, G. E. Scuseria, M. A. Robb, J. R. Cheeseman, G. Scalmani, V. Barone, B. Mennucci, G. A. Petersson, H. Nakatsuji, M. Caricato, X. Li, H. P. Hratchian, A. F. Izmaylov, J. Bloino, G. Zheng, J. L. Sonnenberg, M. Hada, M. Ehara, K. Toyota, R. Fukuda, J. Hasegawa, M. Ishida, T. Nakajima, Y. Honda, O. Kitao, H. Nakai, T. Vreven, J. A. Montgomery Jr., J. E. Peralta, F. Ogliaro, M. Bearpark, J. J. Heyd, E. Brothers, K. N. Kudin, V. N. Staroverov, R. Kobayashi, J. Normand, K. Raghavachari, A. Rendell, J. C. Burant, S. S. Iyengar, J. Tomasi, M. Cossi, N. Rega, N. J. Millam, M. Klene, J. E. Knox, J. B. Cross, V. Bakken, C. Adamo, J. Jaramillo, R. Gomperts, R. E. Stratmann, O. Yazyev, A. J. Austin, R. Cammi, C. Pomelli, J. W. Ochterski, R. L. Martin, K. Morokuma, V. G. Zakrzewski, G. A. Voth, P. Salvador, J. J. Dannenberg, S. Dapprich, A. D. Daniels, Ö. Farkas, J. B. Foresman, J. V. Ortiz, J. Cioslowski and D. J. Fox, *Journal*, 2009.
7. A. A. Peterson, F. Abild-Pedersen, F. Studt, J. Rossmeisl and J. K. Nørskov, *Energy Environ. Sci.*, 2010, **3**, 1311.
8. S. Grimme, *J. Comput. Chem.*, 2006, **27**, 1787.
9. D.-H. Lim, J. H. Jo, D. Y. Shin, J. Wilcox, H. C. Ham and S. W. Nam, *Nanoscale*, 2014, **6**, 5087.